Int. J. Solids Structures, 1968, Vol. 4, pp. 477 to 487. Pergamon Press. Printed in Great Britain

AN ANALYSIS OF VIBRATION EXPERIMENTS THAT APPROXIMATE SIMPLE SHEAR CONDITIONS

JAMES TASI

State University of New York, Stony Brook, New York

Abstract—A three-dimensional isotropic elasticity analysis is used to study vibration experiments that approximate simple shear conditions. A circular disk is analyzed with the conditions that the two parallel faces of the disk are harmonically displaced in opposite directions, and that the cylindrical surface is free of traction. The effect of specimen size on computing shear modulus is quantitatively determined. A simple shear analysis underestimates the true shear modulus, but the error is significant only when the diameter of the specimen is of the order of its thickness. The results for an infinite strip are also given and indicate that a change in specimen shape does not substantially affect the results.

1. INTRODUCTION

A SIMPLE shear test is often a useful means of determining the shear modulus of a continuous medium. However, it is rather difficult, experimentally, to achieve its precise requirements. A block of material, as shown in Fig. 1, must be sheared between two parallel, rigid (or very stiff) planes to produce a linear variation of displacement in the shearing direction, and each point on the bounding surface must experience the same uniform shear stress. If the surface normal to the shearing planes is free of traction, the material actually experiences a state of stress that is neither purely shear nor simple.

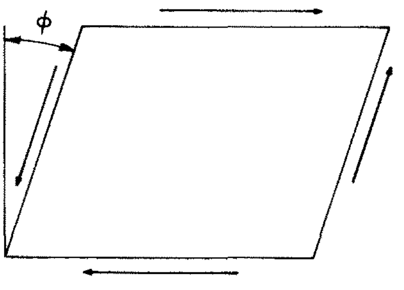

FIG. 1. A block of material, deformed a small angle ϕ, in a state of simple shear.

This situation exists, for example, in the experiments conducted by Fitzgerald [1] to determine the frequency dependence of shear modulus of polymers and crystalline solids.

In the Fitzgerald experiments, one would expect deviations from the simple shear assumption to be manifest only in a boundary layer about the surface that is normal to the shearing planes. Therefore, one can state that for specimens which are much greater in width than they are in thickness the shear modulus obtained will effectively represent a material property. For specimens whose width is of the order of their thickness, however, the shear modulus computed from the simple shear assumption will not be truly a material property but will incorporate the influence of geometry within it.

This paper is concerned with determining the effect of geometry on computing shear modulus with surface conditions appropriate to the Fitzgerald experiments. A three-dimensional isotropic elasticity analysis is used with attention focused on the acoustic frequency range of vibration that is of interest in those experiments. For completeness, one should employ a viscoelastic constitutive equation, especially in the neighborhood of sharp resonance dispersions reported for crystalline solids. However, an elasticity analysis should be conducted first and will at least incorporate the influence of geometry on shear modulus at frequencies below the unique crystalline resonances. The analysis for a circular disk is presented in detail, and the effect of specimen size on computing shear modulus is quantitatively determined. The results for an infinite strip are also given and indicate that a change in specimen shape does not substantially affect the results.

2. ELASTICITY SOLUTION OF SIMPLE SHEAR VIBRATIONS

The displacement equations of motion for an isotropic elastic solid

$$(\lambda+\mu)\nabla(\nabla\cdot\mathbf{u})+\mu\nabla^2\mathbf{u} = \rho\ddot{\mathbf{u}} \tag{1}$$

shall be solved for a circular disk (Fig. 2), subject to the conditions that the top and bottom faces of the disk ($z = \pm h$, where h is the half-thickness of the disk) are harmonically displaced in opposite directions and in a uniform manner. In terms of cartesian or cylindrical

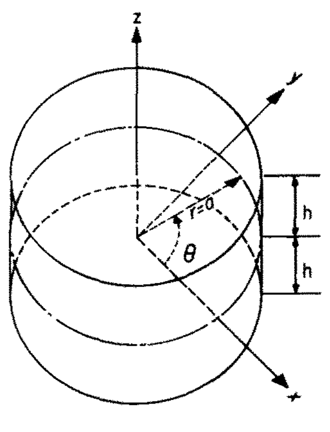

FIG. 2. Geometry of the disk.

coordinates, the conditions at $z = \pm h$ are:

$$\left.\begin{aligned} u_x &= \pm U\,e^{i\omega t} \quad &\text{or}\quad u_r &= \pm U\cos\theta\,e^{i\omega t} \\ u_y &= 0 & u_\theta &= \mp U\sin\theta\,e^{i\omega t} \\ u_z &= 0 & u_z &= 0 \end{aligned}\right\} \tag{2}$$

On the traction free cylindrical surface at $r = a$.

$$\mathbf{t} = \mathbf{e}_r \cdot \boldsymbol{\sigma} = 0 \qquad \text{or} \qquad \begin{cases} \sigma_{rr} = 0 \\ \sigma_{r\theta} = 0 \\ \sigma_{rz} = 0 \end{cases} \tag{3}$$

where $\mathbf{t}$ is the surface traction, $\mathbf{e}_r$ is the radial unit vector and $\boldsymbol{\sigma}$ is the stress dyadic.

It is not possible to obtain a closed form solution to the boundary value problem given by equations (1)–(3). Therefore, a solution shall be obtained which (1) exactly satisfies the equations of motion; (2) exactly satisfies the displacement conditions at $z = \pm h$; (3) approximately satisfies the traction free conditions at $r = a$. First, it is convenient to transform the inhomogeneity in the boundary conditions from the two faces to the cylindrical surface by

$$\mathbf{u}(r, \theta, z, t) = \mathbf{u}^{(0)}(\theta, z, t) + \mathbf{v}(r, \theta, z, t). \tag{4}$$

In (4), $\mathbf{u}^{(0)}(\theta, z, t)$ satisfies the equations of motion and the inhomogeneous conditions at $z = \pm h$, and $\mathbf{v}(r, \theta, z, t)$ satisfies the equations of motion and homogeneous displacement conditions at $z = \pm h$.

The zero-order displacements are

$$\left.\begin{aligned} u_r^{(0)} &= U\frac{\sin(\omega z/c_2)}{\sin(\omega h/c_2)}\cos\theta\, \mathrm{e}^{i\omega t} \\ u_\theta^{(0)} &= -U\frac{\sin(\omega z/c_2)}{\sin(\omega h/c_2)}\sin\theta\, \mathrm{e}^{i\omega t} \\ u_z^{(0)} &= 0 \end{aligned}\right\} \tag{5}$$

with $c_2 = (\mu/\rho)^{\frac{1}{2}}$. As $\omega h/c_2$ approaches zero

$$\left.\begin{aligned} u_r^{(0)} &\to U\frac{z}{h}\cos\theta\, \mathrm{e}^{i\omega t} \\ u_\theta^{(0)} &\to -U\frac{z}{h}\sin\theta\, \mathrm{e}^{i\omega t} \\ u_z^{(0)} &= 0 \end{aligned}\right\} \tag{5'}$$

which is the usual statement of displacements for conditions that approximate simple shear.

The displacement equations of motion are satisfied by requiring the components of $\mathbf{v}$ to be of the form

$$\left.\begin{aligned} v_r &= [A\xi\sin\alpha z - B\beta\sin\beta z]J_1'(\xi r)\cos\theta\, \mathrm{e}^{i\omega t} \\ &\quad + C\sin\gamma z\frac{J_1(\eta r)}{\eta r}\cos\theta\, \mathrm{e}^{i\omega t} \\ v_\theta &= -[A\xi\sin\alpha z - B\beta\sin\beta z]\frac{J_1(\xi r)}{\xi r}\sin\theta\, \mathrm{e}^{i\omega t} \\ &\quad - C\sin\gamma z J_1'(\eta r)\sin\theta\, \mathrm{e}^{i\omega t} \\ v_z &= [A\alpha\cos\alpha z + B\xi\cos\beta z]J_1(\xi r)\cos\theta\, \mathrm{e}^{i\omega t} \end{aligned}\right\} \tag{6}$$

with

$$\alpha^2 = \omega^2/c_1^2 - \xi^2$$
$$\beta^2 = \omega^2/c_2^2 - \xi^2$$
$$\gamma^2 = \omega^2/c_2^2 - \eta^2$$

and

$$c_1 = [(\lambda + 2\mu)/\rho]^{\frac{1}{2}}.$$

In equations (6), the dependence on z associated with coefficients A and B is identical to that in the plane strain solution for straight crested antisymmetric waves in an infinite plate [2]. The terms with coefficient C represent displacements due to rotational waves about the z direction. Superposition of the two classes of displacements yields the general solution for $\mathbf{v}$.

The application of

$$v_r = v_\theta = v_z = 0, \qquad \text{at } z = \pm h \tag{7}$$

yields wave numbers governed by

$$\gamma h = n\pi, \qquad n = 1, 2, 3, \ldots \tag{8}$$

and

$$\frac{(\xi h)^2}{(\alpha h)(\beta h)} + \frac{\tan \beta h}{\tan \alpha h} = 0 \tag{9}$$

with

$$\frac{A}{B} = -\frac{\xi h}{\alpha h}\frac{\cos \beta h}{\cos \alpha h}.$$

Before proceeding further, one must recognize that equation (9) is in a form unsuitable for numerical calculations within the acoustic range of frequencies. An expansion of equation (9) in powers of ω^2 with the condition

$$\omega \ll c_2/h \quad \text{(acoustic frequencies)}$$

yields the secular equation

$$\sinh(2\zeta) + 2\zeta\frac{(1 - 1/k^2)}{(1 + 1/k^2)} = 0. \tag{9'}$$

The solutions for $\mathbf{v}$ must be modified in a similar manner, with the result

$$\left.\begin{aligned}
v_r &= A\left\{\left(1+\frac{1}{k^2}\right)\frac{\sinh(\zeta\bar{z})}{\cosh\zeta}+\zeta\left(1-\frac{1}{k^2}\right)\left[\bar{z}\frac{\cosh(\zeta\bar{z})}{\cosh\zeta}-\tanh\zeta\frac{\sinh(\zeta\bar{z})}{\cosh\zeta}\right]\right\} \\
&\quad\cdot\frac{J'_1\left(\zeta\frac{a}{h}\bar{r}\right)}{J_1\left(\zeta\frac{a}{h}\right)}\cos\theta\, e^{i\omega t}+C\frac{\sin(n\pi\bar{z})J_1\left(in\pi\frac{a}{h}\bar{r}\right)}{\left(n\pi\frac{a}{h}\bar{r}\right)J_1\left(in\pi\frac{a}{h}\right)}\cos\theta\, e^{i\omega t} \\
v_\theta &= -A\left\{\left(1+\frac{1}{k^2}\right)\frac{\sinh(\zeta\bar{z})}{\cosh\zeta}+\zeta\left(1-\frac{1}{k^2}\right)\left[\bar{z}\frac{\cosh(\zeta\bar{z})}{\cosh\zeta}-\tanh\zeta\frac{\sinh(\zeta\bar{z})}{\cosh\zeta}\right]\right\} \\
&\quad\cdot\frac{J_1\left(\zeta\frac{a}{h}\bar{r}\right)}{\left(\zeta\frac{a}{h}\bar{r}\right)J_1\left(\zeta\frac{a}{h}\right)}\sin\theta\, e^{i\omega t}+C\frac{\sin(n\pi\bar{z})J'_1\left(in\pi\frac{a}{h}\bar{r}\right)}{iJ_1\left(in\pi\frac{a}{h}\right)}\sin\theta\, e^{i\omega t} \\
v_z &= A\left\{\zeta\left(1-\frac{1}{k^2}\right)\left[\frac{\bar{z}\sinh(\zeta\bar{z})}{\cosh\zeta}-\tanh\zeta\frac{\cosh(\zeta\bar{z})}{\cosh\zeta}\right]\right\}\frac{J_1\left(\zeta\frac{a}{h}\bar{r}\right)}{J_1\left(\zeta\frac{a}{h}\right)}\cos\theta\, e^{i\omega t}.
\end{aligned}\right\}\qquad(10)$$

In equations (9′) and (10), $\zeta = \xi h$, $k = c_1/c_2$, $\bar{z} = z/h$ and $\bar{r} = r/a$. Also, the displacements are scaled for convenience in calculation.

Equation (9′) and the spatial terms in (5′) and (10) are precisely the solutions that would be found if one had attempted a static analysis [3] to begin with, rather than a dynamic analysis. Although a static solution for the spatial variation of displacements does not satisfy the equations of motion, the error involved is negligible.*

The secular equation given by (9′) does not allow real or imaginary roots. Only complex roots and their complex conjugates are possible. The double infinity of wave numbers ζ and ζ^*, with the infinity of wave numbers provided by equation (8), add up to a triple infinity of possible solutions to $\mathbf{v}$. The complete set of displacements can be represented by

$$\mathbf{v} = \left[\sum_{n=1}^{\infty} A_n\mathbf{v}_\zeta^{(n)}+\sum_{n=1}^{\infty} A_n^*\mathbf{v}_\zeta^{(n)*}+\sum_{n=1}^{\infty} C_n\mathbf{v}_\gamma^{(n)}\right]e^{i\omega t}\qquad(11)$$

where $\mathbf{v}_\zeta^{(n)}$ indicates displacements corresponding to the nth value of ζ, $\mathbf{v}_\gamma^{(n)}$ indicates displacements corresponding to the nth value of γ and an asterisk denotes a complex conjugate.

The coefficients A_n, A_n^*, C_n are determined by requiring the three stress conditions at $r = a$ to be satisfied. Let $\boldsymbol{\sigma}^{(0)}$ and $\boldsymbol{\tau}$ be the stresses calculated from $\mathbf{u}^{(0)}$ and $\mathbf{v}$, respectively.

* There are two physical discrepancies between conditions in the Fitzgerald apparatus and the analysis. First, an initial axial stress state is applied by the apparatus to clamp a specimen. However, if the initial stress is much less than the shear modulus, as it must be for real materials, it can be shown that the initial stress will not influence the numerical results. Second, in the experiments, the bottom face is essentially stationary; only the top face is displaced. To accommodate this, one should add a symmetric solution to the antisymmetric displacements presented in this section. The symmetric solution, however, is of the order of the high frequency terms that are unimportant for acoustic frequencies.

The traction free condition given by (3) is then

$$\mathbf{t} = \mathbf{e}_r \cdot (\boldsymbol{\sigma}^{(0)} + \boldsymbol{\tau}) = 0$$

or

$$\left.\begin{aligned} \tau_{rr} &= 0 \\ \tau_{r\theta} &= 0 \\ \tau_{rz} &= -\sigma_{rz}^{(0)} = -\mu \frac{U}{h} \cos\theta\, e^{i\omega t}. \end{aligned}\right\} \tag{12}$$

The algorithm we shall use to calculate the unknown coefficients is simply a direct use of Hamilton's Principle. The procedure has been suggested by Mindlin [4] and used with good effect by Onoe [5]. Instead of applying it to the real, physical displacement $\mathbf{u}$, however, we shall apply it to the reduced displacement $\mathbf{v}$ with associated boundary conditions given by equations (7) and (12).

For harmonic vibrations, Hamilton's Principle reduces to

$$\int_V (-\omega^2 \rho \mathbf{v} - \nabla \cdot \boldsymbol{\tau}) \cdot \delta \mathbf{v}\, dV - \int_S (\mathbf{t}^{(0)} - \mathbf{n} \cdot \boldsymbol{\tau}) \cdot \delta \mathbf{v}\, dS = 0$$

in which integration with respect to time has been carried out over a cycle of vibration and only spatial components of the variables remain. Since each term in $\mathbf{v}$ in equation (11) satisfies the equations of motion, the volume integral is identically zero. Since $\delta \mathbf{v} = 0$ at $z = \pm h$, the surface integral reduces to

$$\int_{S_c} (\mathbf{t}^{(0)} - \mathbf{e}_r \cdot \boldsymbol{\tau}) \cdot \delta \mathbf{v}\, dS_c = 0 \tag{13}$$

where S_c is the cylindrical surface. Substituting the spatial components of equation (11) and

$$\mathbf{t}^{(0)} = -\sigma_{rz}^{(0)} \mathbf{e}_z$$

into (13), and reversing the order of summation and integration, we obtain a triple infinity of linear inhomogeneous algebraic equations governing the coefficients. The equations are symmetric, complex, and can be solved in truncated form.

The analysis used to obtain shear modulus (say, $\bar{\mu}$) using a simple shear approximation is simply

$$\bar{\mu} = \frac{T}{\pi a^2 (U/h)}$$

where T is the amplitude of the total shear force applied to one face of the specimen. In terms of the elasticity analysis, however,

$$T e^{i\omega t} = \int_A (\sigma_{zx})_{z=h}\, dx\, dy$$
$$= \int_0^a \int_0^{2\pi} (\sigma_{zr} \cos\theta - \sigma_{z\theta} \sin\theta)_{z=h} r\, dr\, d\theta$$

and yields

$$\frac{T}{\pi a^2(U/h)} = \mu\left[1 + \frac{2}{a/h}\sum_{n=1}^{\infty}\frac{(A_n + A_n^*)}{U} + \frac{1}{a/h}\sum_{n=1}^{\infty}(-1)^n\frac{C_n}{U}\right].$$

The ratio of shear modulus obtained from a simple shear approximation to the true shear modulus is, therefore,

$$\frac{\bar{\mu}}{\mu} = \left[1 + \frac{2}{a/h}\sum_{n=1}^{\infty}\frac{(A_n + A_n^*)}{U} + \frac{1}{a/h}\sum_{n=1}^{\infty}(-1)^n\frac{C_n}{U}\right]. \tag{14}$$

In equation (14), the influence of geometry on the difference between the two moduli is directly shown by the ratio a/h, but its influence, and the influence of Poisson's ratio, is also incorporated indirectly in the coefficients A_n, A_n^*, and C_n.

3. NUMERICAL RESULTS

Asymptotic expressions for the complex roots of (9′) are

$$\left.\begin{aligned}\operatorname{Re}\zeta &= \tfrac{1}{2}\ln[4b\pi(n-\tfrac{1}{4})]\\ \operatorname{Im}\zeta &= \pi(n-\tfrac{1}{4})\end{aligned}\right\} n = 1, 2, 3, \ldots$$

where

$$b = \frac{(1-1/k^2)}{(1+1/k^2)} = \frac{1}{(3-4\nu)}$$

and ν is Poisson's ratio. Correct numerical values for the roots are then determined by applying Newton's method [6] to the real and imaginary parts of equation (9′), with the asymptotic expressions used as first estimates. Only two or three iterations are required to achieve six figure accuracy.

In the truncated equations obtained from (13), an equal number of wave numbers are retained for ζ, ζ^*, and γh, in order to keep $\mathbf{v}$ real and to maintain the same magnitude of spatial attenuation in the components of equation (11). Although the sum of terms in $\mathbf{v}$ is real, it is convenient to use the complex form of the first two series in (11). The solution of the truncated equations by Crout reduction was carried out by an IBM 7090 computer, using its built in subroutine for complex algebra. In the results that follow, eighteen simultaneous equations were used.

Figures 3–6 illustrate solutions for $a/h = 2$. Figures 3 and 4 indicate the magnitude of the stresses σ_{rz}, σ_{rr} that remain on the cylindrical surface due to truncation ($\sigma_{r\theta}$ is too small to plot). Note that the solution is deficient at ($z = \pm h$, $r = a$) because of the singularity imposed by the boundary conditions. The nature of the stresses on a sheared face of the disk is indicated in Fig. 5. An antisymmetric distribution of axial stress σ_{zz}, with large magnitude near the cylindrical boundary, is required to maintain the equilibrium

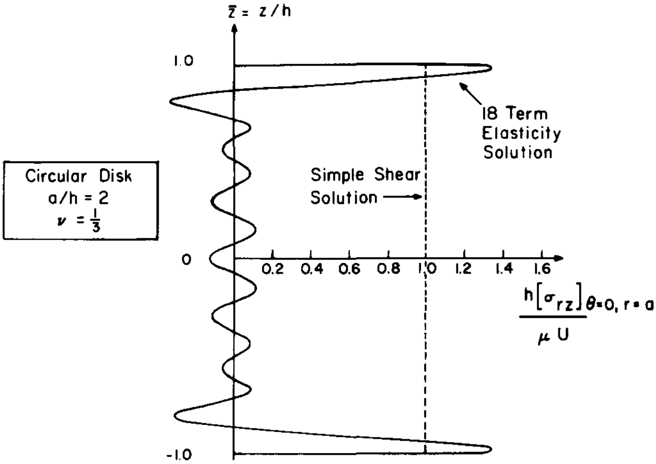

FIG. 3. Amplitude of stress σ_{rz} remaining on the cylindrical boundary; $a/h = 2$, $\nu = \frac{1}{3}$.

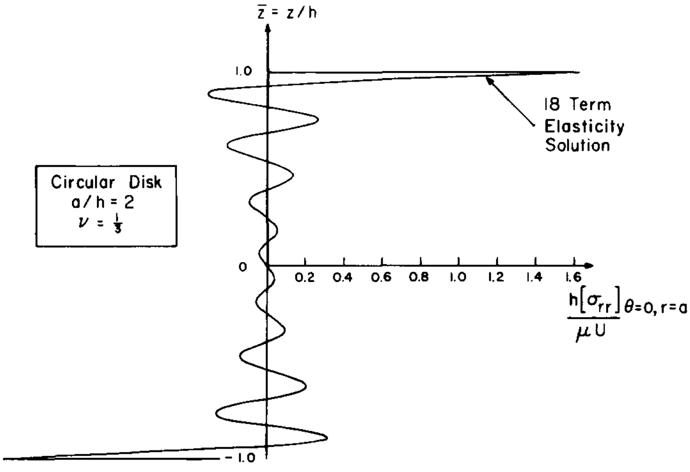

FIG. 4. Amplitude of stress σ_{rr} remaining on the cylindrical boundary; $a/h = 2$, $\nu = \frac{1}{3}$.

of the disk. The distribution of u_x at ($x = a$, $y = 0$) is given in Fig. 6, and closely approximates a linear, simple shear distribution.

The variation of $\bar{\mu}/\mu$ with diameter to thickness ratio is given in Fig. 7 for Poisson's ratios of 1/3 and 1/2. The modulus obtained from a simple shear calculation is always smaller than the true modulus, with noticeable error when a/h is of the order of unity. The influence of the residual traction that has not been eliminated from the cylindrical surface is indicated by the ratio of the moment (M_r) about the y axis contributed by the residual traction to the moment (M_a) about the y axis provided by the applied shear stresses on the two faces of the disk. For simple shear, M_r/M_a is unity. For a traction free surface at $r = a$, M_r/M_a is zero. The smallness of the ratio is a quantitative estimate of how well the truncated solution approximates the boundary conditions posed by

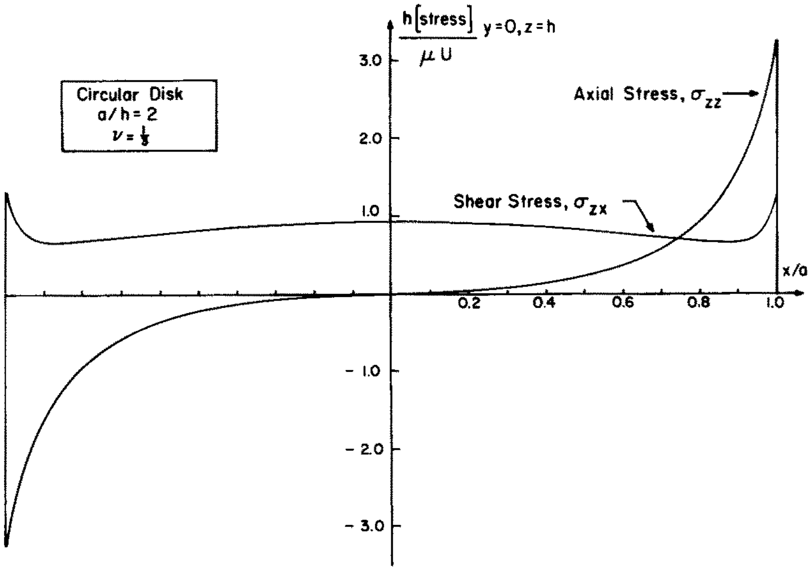

FIG. 5. Amplitude of axial and shear stresses on a face of the disk; $a/h = 2$, $\nu = \frac{1}{3}$.

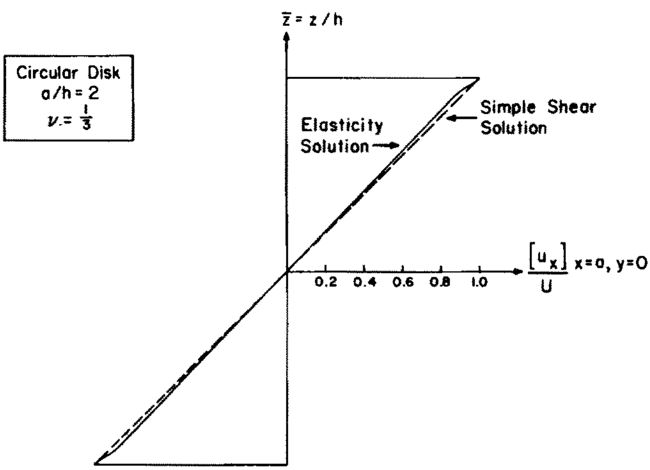

FIG. 6. Amplitude of displacement u_x on the cylindrical boundary; $a/h = 2$, $\nu = \frac{1}{3}$.

equation (3). The results are generally satisfactory. Moreover, $\bar{\mu}/\mu$ converges quite rapidly and its convergence is found to be less sensitive to the residual tractions than is M_r/M_a.

Finally, in Fig. 8, $\bar{\mu}/\mu$ for an infinite strip $(-a \leq x \leq a, -\infty < y < +\infty)$ is compared to the values obtained for a circular disk. The difference is quite small, indicating that a change in specimen shape does not substantially affect the results. Read [7] has provided upper and lower bounds for the infinite strip results presented here, as well as the appropriate energy arguments for requiring that the simple shear modulus be less than the actual shear modulus.

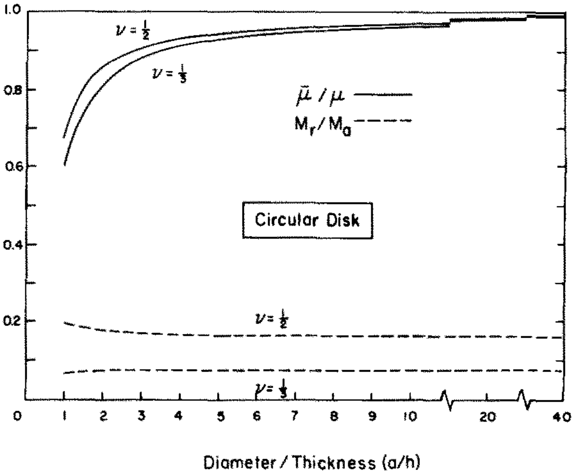

FIG. 7. Ratio of shear modulus obtained for simple shear approximation to true shear modulus ($\bar{\mu}/\mu$) vs. diameter to thickness ratio for circular disk; $\nu = \frac{1}{3}$ and $\frac{1}{2}$. Also M_r/M_a vs. diameter to thickness ratio.

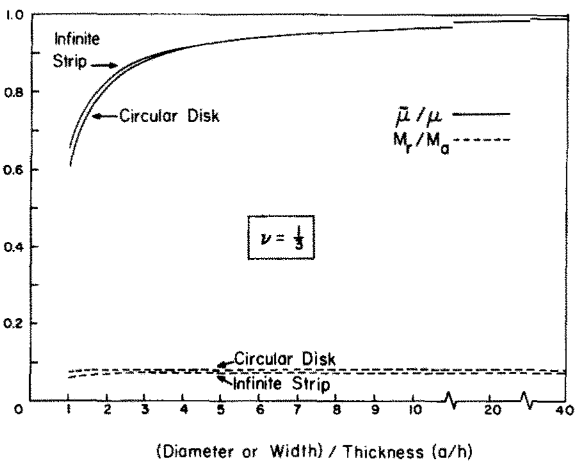

FIG. 8. $\bar{\mu}/\mu$ vs. diameter to thickness ratio for a circular disk or width to thickness ratio for an infinite strip; $\nu = \frac{1}{3}$. Also, M_r/M_a for circular disk and infinite strip.

4. CONCLUSIONS

The analysis of a simple shear vibration test, when applied to a linear isotropic elastic material, indicates that:

1. Within the acoustic range of frequencies, a static solution for the spatial variation of displacement involves negligible error.

2. If shear stress is applied solely to two parallel faces, a simple shear analysis underestimates the true shear modulus. The error is only significant, however, when the diameter (or width) of the specimen is of the order of its thickness. For example, with Poisson's ratio equal to $\frac{1}{3}$, the simple shear elastic modulus for diameter to thickness ratio equal to 4 is in error by 8 percent, and for a diameter to thickness ratio of unity the modulus is in error by 40 percent. The error is less for an incompressible solid.

3. Specimen shape appears to be unimportant.

Acknowledgements—The author would like to thank Professor Edwin R. Fitzgerald for his valuable discussions of the subject.

Most of this work was performed while the author was a Post-Doctoral Fellow at The Johns Hopkins University, with support from the Sloan Foundation and Office of Naval Research (Acoustics Programs).

REFERENCES

[1] E. R. Fitzgerald, *Developments in Mechanics*, Vol. 1. Plenum Press (1961).
[2] R. D. Mindlin, *Proc. 1st Symp. on Naval Structural Mechanics*. Pergamon Press (1960).
[3] A. E. Green, *Proc. R. Soc.* **A195**, 533 (1949).
[4] R. D. Mindlin, *Investigations in the Mathematical Theory of Vibrations of Anisotropic Bodies*. Columbia University Report No. CU-4-56-SC-64687-CE (1956).
[5] M. Onoe, *J. acoust. Soc. Am.* **30**, 1159 (1958).
[6] F. B. Hildebrand, *Introduction to Numerical Analysis*. McGraw-Hill (1956).
[7] W. T. Read, *J. appl. Mech.* **17**, 349 (1950).

(*Received* 15 *May* 1967; *revised* 21 *August* 1967)

Абстракт При исследовании вибрационных экспериментов, которые приближают простые условия сдвига используется трехмерная изотропная задача упругости. Рассматриваетсн круглой диск с такими условиями, что две параллелвные поверхности диска перемещаются в противоположенных направлениях и, что цилиндрическая поверхностъ свободна от усилий. Определяется, количественно, зффект размера образща на расчет модула сдвига. Простая задача сдвига оценивает слишком низко действителвный модулъ сдвига, но погрешхностъ имеет значение толъко тогда, когда порядок диаметра образца равен порядку его толщины. Приводятся также резулътаты для бесконечной полосы. Приводятся также резулътаты для бесконечной полосы. Они указывают, что изменение формы образца не влияет, в основ, на резулътаты.